Low-GWP Working Fluid Mixtures Screening for Industrial High Temperature Heat Pumps with Supply Temperature >200 °C

Conference Paper · July 2024

4 authors:

Jan Špale
Czech Technical University in Prague

Andreas Hoess
Purdue University

Ian H. Bell
National Institute of Standards and Technology

Davide Ziviani
Purdue University

Low-GWP Working Fluid Mixtures Screening for Industrial High Temperature Heat Pumps with Supply Temperature >200 °C

Jan SPALE[1, 2]*, Andreas J. HOESS[2], Ian H. BELL[3], Davide ZIVIANI[2]

[1] Purdue University,
Ray W. Herrick Laboratories, School of Mechanical Engineering,
177 S Russell St, West Lafayette, IN 47907, USA
dziviani@purdue.edu

[2] Czech Technical University in Prague,
University Center for Energy Efficiency Buildings,
Jugoslavskych partyzanu 1580/3, 160 00 Prague, Czech Republic
jan.spale@cvut.cz

[3] National Institute of Standards and Technology,
Applied Chemicals and Materials Division,
Boulder, CO 80305, USA
ian.bell@nist.gov

* Corresponding Author

ABSTRACT

Single-component working fluids, which could be used in a safe, efficient, reliable, and cost-effective industrial high temperature heat pump (HTHP) subcritical vapor-compression cycle (VCC) for process heat delivery at 200 °C are scarce and come with significant technical limitations. We therefore propose searching for a mixture that could meet these criteria.

Hence, we created a Python code using REFPROP and Cantera libraries to model a simplified HTHP VCC with an advanced cycle architecture and to assess the flammability of the mixture. Ten single-component fluids consisting of two subsets – hydrocarbons and hydro(chloro)fluoroolefins – were identified. From these, over 460,000 binary, ternary and quaternary mixtures were created. Solving the advanced HTHP VCC for each, we obtained cycle performance results which we filtered and sorted using thermodynamic and technical criteria. We did not find a perfect mixture which would meet all our criteria but a binary blend of cyclopentane and R1336mzz(Z) with mole fraction of [0.68,0.32] was selected as the winner candidate of the screening given the imposed limits. This mixture will be further experimentally investigated and used in a purpose-built test rig for HTHP screw compressor development. This work is a shortened version of a more extensive journal publication currently under review at the time of this conference manuscript submission. (Spale et al., 2024a)

1. INTRODUCTION

The decarbonization of energy intensive industries is a major step that needs to be taken to pursue a carbon neutral economy by the middle of this century. This results mostly in a technology shift from fossil fuel driven processes to fully electrified solutions. Industrial high temperature heat pumps are a key enabling technology for this energy transition as they enable the electrification of low temperature process heat supply, increase process heating system efficiency, reduce the carbon footprint of production processes, recover waste heat, provide sector coupling, allow for flexibility, aggregation, and provide grid ancillary services on the demand side.

In designing a system to operate with condensing temperature of 200 °C, we face the challenge of finding suitable single-component working fluids since most synthetic refrigerants have lower critical temperatures, leaving natural refrigerants as the primary viable option in this uncharted territory for subcritical systems. Looking at the number of available working fluids in REFPROP 10 (E. W. Lemmon et al., 2018) in terms of being able to operate in a subcritical

VCC (applying a limit of $T_{cond} < 0.95T_{crit}$), there are fewer than 50 fluids available, out of which most are not suitable to operate as working fluids in a VCC due to safety hazards or technical constraints in terms of operating pressures and thermal and chemical stability. The compounds that survive this pre-selection are alcohols, siloxanes, higher hydrocarbons (long-chain alkanes or cyclic hydrocarbons), some of the banned and phased-out CFCs (e.g. R113) and water. Among these compounds, higher hydrocarbons stand out as promising candidates. However, using pure hydrocarbons presents difficulties, including low vapor pressure requiring airtight systems potentially requiring a purge system, high flammability posing explosive risks, high compressor discharge temperatures challenging compressor oil development, and low volumetric heating capacity (VHC) requiring large and therefore more costly equipment. One of the options to work around is to blend a mixture of multiple pure fluid components. Blending a multi-component blend gives an additional degree of freedom to find a tradeoff between often conflicting qualities such as high VHC and high COP or between low GWP and flammability.

In the area of working fluid mixtures screening for HTHP systems with above 165 °C heat supply, there have been multiple previous efforts. (Abedini et al., 2023; Fernández-Moreno et al., 2022; Ganesan & Eikevik, 2023; Obika et al., 2024) We propose to blend a natural refrigerant – higher hydrocarbon – with an H(C)FO. This aspires to overcome shortcomings of pure fluids in this temperature range while meeting targets for environmental hazard, toxicity, flammability, and performance requirements at subcritical VCC operation. Therefore, we perform an exploratory study of potential working fluid mixtures of HCs and H(C)FOs for such an industrial HTHP system.

2. METHODOLOGY AND MODEL DESCRIPTION

The exploration of a working fluid for a 200 °C supply temperature involved the following steps:

1) Pre-select the list of higher hydrocarbons as the main components of the mixture and the list of low-GWP zero-ODP non-flammable high T_{crit} pure H(C)FOs as other components of the mixture.
2) Perform the advanced HTHP VCC calculation for each of the variation of mixtures – binary up to quaternary.
3) Determine the mixture performance indicators for all variations of mixtures – thermodynamic performance: COP, VHC, 2nd law efficiency, compressor flow rate, pressure ratio, vapor pressure and flammability.
4) Evaluate the mixtures using custom filter and sort functions and select the most suitable mixture for given case and user's sensitivity to each parameter (later called "best").

2.1 Working Fluids Pre-selection

Two groups of fluids were manually selected for mixture screening. The way the pre-selected fluids to the fluid list were narrowed down consisted of a combination of thermodynamic criteria as well as recommendations from the industry and earlier attempts in the available literature. Values in Table 1 are obtained from REFPROP (E. W. Lemmon et al., 2018) and from the WMO Ozone report. (World Meteorological Organization (WMO), 2022)

Table 1 Pre-selected pure fluid components of the mixture

Fluid	T_{crit} (°C)	p_{crit} (kPa)	$p_{vap}^{25°C}$ (kPa)	GWP_{100} (-)	ODP (-)	A34† (-)	NBP†† (°C)	MW ($g \cdot mol^{-1}$)	T_{freez} (°C)
toluene	318.60	4126	3.80	<< 1*	0	A3	110.6	92.14	-95.15
cyclohexane	280.45	4081	13.02	-	0	A3	80.70	84.16	6.71
cyclopentane	238.57	4583	42.34	<< 1*	0	A3	49.25	70.13	-93.45
benzene	288.87	4907	12.70	<< 1*	0	A3	80.06	78.11	5.52
acetone	234.95	4692	30.73	< 1**	0	A3	56.07	58.08	-94.65
R1336mzz(E)	137.70	3157	193.43	26	0	A1	7.50	164.06	-73.00
R1336mzz(Z)	171.35	2903	73.56	2	0	A1	33.45	164.06	-90.50
R1233zd(E)	166.45	3624	129.81	4	~0	A1	18.26	130.50	-78.00
R1224yd(Z)	155.54	3337	148.52	< 1**	~0	A1	14.62	148.49	-10.15
R1234ze(Z)	150.12	3531	177.48	< 1**	0	A2L	9.73	114.04	-35.15

* GWP_{100} values that are less than 0.1
** GWP_{100} values between 0.1 and 1
† A34 is an abbreviation for the safety group classification by the ASHRAE 34 Standard (ASHRAE, 2022)
†† NBP is an abbreviation for normal boiling point defined as the temperature at which the vapor pressure of a liquid is equal to the atmospheric pressure

2.2 HTHP Cycle Model for Working Fluid Mixtures Screening

The steady state HTHP model is based on heat and mass balance and was built in Python using the REFPROP 10 library for thermodynamic properties calculations. (E. W. Lemmon et al., 2018) Architecture of the mixture screening code is based on the work of (Bell et al., 2019), but adapted for HTHPs and extended. The HTHP model uses a secondary pressurized water loop to deliver heat to the evaporator. This heat input emulates a high temperature industrial waste heat stream. A customized screw compressor with a vapor injection is utilized. The heat sink secondary loop uses a standard thermal oil heat transfer fluid. The cycle schematic is shown in Figure 1 below and presents a simplified version of an advanced two-stage economized cycle with an internal heat exchanger, a promising cycle architecture for very high temperature heat supply. (Mateu-Royo et al., 2021) The Python tool allows to quickly evaluate also other cycle configurations and architectures, although for the sake of simplicity, only this architecture is explored within this study. The boundary conditions of the modelled cycle are listed below in Table 2 and are selected with respect to the technical configuration and limitations of the laboratory setup as the cycle with the "best" mixture will be experimentally verified.

The following assumptions were employed:

- Thermal and pressure losses are neglected.
- Compressor isentropic efficiency is a function of pressure ratio using (Eq. 2.).
- Volumetric efficiency as well as motor electrical efficiency and drivetrain mechanical efficiency of 1 is assumed.
- Heat exchangers are modelled as counterflow using a pinch point analysis with constant minimum approach temperature difference and discretization.
- Expansion valves assume isenthalpic processes.
- 5 K superheat assumed at economized vapor injection.

Using these assumptions, the cycle model is solved iteratively by initially guessing the non-dimensional mass flow rate in the economizer branch α_{split} (see the splitter node in Figure 1 for reference) and solving for the desired economizer superheat controlling the non-dimensional mass flow rate for the main (1-α_{split}) and split flow (α_{split}) branches (see Eq. 1).

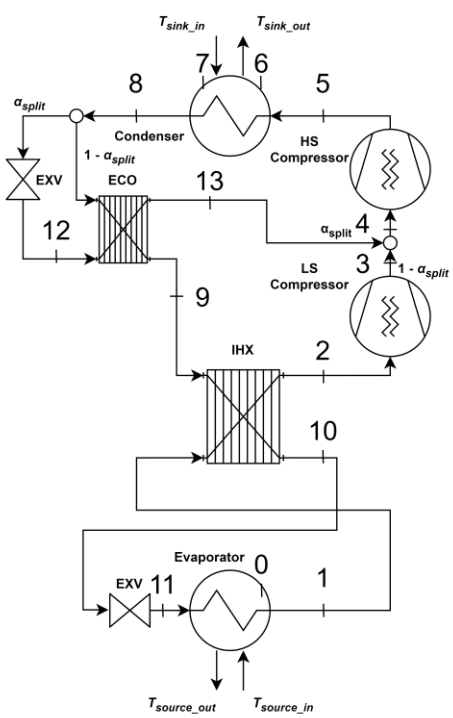

Figure 1 Cycle schematics of the high temperature heat pump model

Table 2 Boundary conditions of the investigated cycle

Parameter	Value	Unit
Heat source inlet temperature $T_{source_{in}}$	120	°C
Heat sink inlet temperature $T_{sink_{in}}$	174	°C
Evaporator dew point temperature T_{ev}	110	°C
Condenser bubble point temperature T_{cond}	200	°C
Evaporator superheat ΔT_{SH}	5	K
Condenser subcooling ΔT_{SC}	5	K
Condenser minimum temperature difference $\Delta T_{cond_{min}}$	3	K
Evaporator minimum temperature difference $\Delta T_{ev_{min}}$	3	K
Economizer minimum temperature difference $\Delta T_{eco_{min}}$	25	K
IHX minimum temperature difference $\Delta T_{IHX_{min}}$	25	K
Heating capacity Q_{cond}	100	kW

2.3 Screening Methodology

First, the code reads the boundary conditions of the cycle, type of cycle architecture, heat sink and source parameters and the list of fluids pre-selected for the analysis. Next, the code generates all the possible variations of mixture compositions from the fluids list (repetitions are excluded) either for binary, ternary or quaternary mixtures with a 4% mole fraction step size. As the next step, in parallel, for each mixture, the HTHP cycle is calculated using the multiprocessing module for Python. (*Multiprocessing — Process-Based Parallelism*, 2024)

Please refer to Figure 1 for the corresponding state point subscripts. The cycle subfunction first initializes the parameters for REFPROP mixture calculations and calculates GWP_{100} of the mixture. Then it continues with getting critical parameters of the mixture and vapor pressure at 25 °C. To achieve the condition of injecting 5 K superheated vapor to the screw compressor, the α_{split}, economizer split flow non-dimensional mass flow rate (branch 12-13), is iterated and so is the calculation of every state property with it. A convergence criterium assumes h_{13} to be within 0.1 $kJ \cdot kg^{-1}$ tolerance field of the objective state superheated to the desired superheat above the mid-pressure dew point – see (Eq. 1). This equation is then solved for α_{split} by minimizing the difference between h_{13} and h_{obj} using a L-BFGS-B method. (*Scipy.Optimize.Minimize — SciPy v1.12.0 Manual*, 2024)

$$h_{13} = \frac{\alpha_9}{\alpha_{12}} \cdot (h_8 - h_9) + h_{12} = h_{obj}(p_{12}; T(p_{12}; x = 1) + \Delta T_{SH}) \tag{1}$$

The isentropic efficiency of the screw compressor is calculated using the following function (Eq. 2) of pressure ratio π obtained for a high temperature screw compressor from (Ganesan & Eikevik, 2023) as an initial estimate for sizing of the system. This function will be updated by the compressor efficiency map once one is obtained from the experimental testing.

$$\eta_{\text{is}} = -0.00000461\pi^6 + 0.00027131\pi^5 - 0.00628605\pi^4 + 0.07370258\pi^3 - 0.46054399\pi^2 + 1.40653347\pi - 0.87811477 \tag{2}$$

Other state points are determined using REFPROP based on known state properties from the boundary conditions. If wet compression should occur in the screw compressor (2-3 or 4-5) with the given boundary condition, such mixture is discarded from the results and the screening proceeds with the next mixture. After the α_{split} solver converges, mass flow rate of the refrigerant is calculated from the $\dot{Q}_{\text{cond}}$ heating capacity boundary condition and the heat source and heat sink side are calculated using the pinch point analysis with discretization of the heat exchangers into 100 elements. Finally, mass flow rates of the sink and source fluids are calculated using heat and mass balance of the evaporator and condenser respectively. The intermediate pressure level is estimated using the geometric mean of the condensing and evaporating pressures as a preliminary estimate in order to save computational resources instead of an additional optimization loop for cycle performance.

Next up, cycle benchmark parameters are calculated. For comparison of different mixtures, COP of the heat pump (Eq. 3), volumetric heating capacity (VHC) (Eq. 4) and second law efficiency (Eq. 5) are used.

$$\text{COP} = \frac{q_{cond}}{w_{comp_{LS}} + w_{comp_{HS}}} = \frac{\alpha_5 \cdot (h_5 - h_8)}{(\alpha_2 \cdot (h_3 - h_2)) + (\alpha_4 \cdot (h_5 - h_4))} \ (-) \tag{3}$$

$$\text{VHC} = q_{cond} \cdot \rho_2 \cdot 10^6 = \alpha_5 \cdot (h_5 - h_8) \cdot \rho_2 \cdot 10^6 \ (\text{MJ} \cdot \text{m}^{-3}) \tag{4}$$

$$\eta_{2nd} = \frac{\text{COP}}{\text{COP}_{\text{Carnot}}} = \frac{\dfrac{q_{cond}}{w_{comp_1} + w_{comp_2}}}{\dfrac{T_{sink_{out}}}{T_{sink_{out}} - T_{source_{in}}}} \ (-) \tag{5}$$

Finally, the results from the cycle model then get saved into a dictionary of outputs and this is passed back upstream, where all the dictionaries from all the mixtures are compiled into a single data frame object for further post-processing of the results.

The flammability estimation model is a separate script which reads the compiled data frame object from the cycle model and performs the flammability estimation of the mixture for each. Flammability calculations are performed

using the Cantera open source kinetic solver and the NASA7 polynomials for the calculation of the ideal gas properties of the species and elements. (Goodwin et al., 2021) The method of estimating the flammability of the mixture follows the methodology by (Linteris et al., 2019) The key two parameters to estimate the ASHRAE Standard 34 classification (ASHRAE, 2022) of the resulting mixture are the molar F/(F+H) ratio (number of fluorine atoms over sum of hydrogen and fluorine atoms known as fluorine loading) and the maximum adiabatic flame temperature in reaction with air varying the fuel-air ratio. The thermo mechanism for species and elements used for the kinetic equations was constructed using the open-source RMG tool. (Gao et al., 2016)

After the flammability estimation parameters are calculated, the data are evaluated in post-processing. This includes filtering and sorting the resulting data using the pandas library. (*Pandas Documentation — Pandas 2.2.1 Documentation*, 2024) The choice of the filter criteria is based on multiple aspects such as technical limitations of the equipment or desired thermodynamic performance. These are:

- heat sink supply temperature $T_{sink_{out}}$ above 200 °C.
- compressor discharge temperature T_5 below 220 °C (excessive compressor discharge temperatures may create difficulties in managing the compressor's heat and in the development of lubricants, gaskets and seals for the screw compressor; this constraint is contingent upon significant upcoming R&D efforts in this field, and is for sure amongst the greatest challenges of the HTHP development)
- vapor pressure $p_{vap}^{25°C}$ above 50 kPa(a) – a design constraint coming from the discussions with the industrial partners for an open-drive screw compressor.
- 2nd law efficiency η_{2nd} based on COP_{Carnot} above 0.5.
- critical temperature T_{crit} above 210 °C (10 K above bubble point temperature)

Finally, the data are sorted by second law efficiency (largest -> smallest) and thus the preferred mixture is selected.

3. RESULTS OF WORKING FLUID MIXTURES SCREENING

In total 468,330 binary, ternary and quaternary mixture variations derived from the pure components listed in Table 2 were analyzed. For this large dataset of mixtures, cycle parameters were calculated using the model described in Section 2. The next, and in a sense more difficult part, was to weigh the figures of merit and decide on the filtering criteria and sorting parameters based on the technical limitations. Figure 2 presents a graphical representation of the screening results in hexbin histogram charts where the colorscale represents frequency of occurrence of the results in a grid consisting of hexagonal bins. The results in this section are presented for clarity and completeness only for the ternary mixtures, although calculations were made separately for binary, ternary and quaternary mixtures. Results for each subset can be found in the separate dataset published in (Spale et al., 2024b).

3.1 Mixtures Screening Results and Filtering

When the screening process is completed, out of 42,120 initial ternary compositions, 24,371 mixtures are left. Some have critical temperature lower than the condensing temperature, others would end up with a compression in a wet vapor region. Such fluids are skipped and the screening proceeds with another mixture composition. Figure 2a) shows the COP of these mixtures as a function of VHC, which is a useful plot to better understand what regions these mixtures cover. Ideally, COP and VHC should be both maximized while other filtering criteria are met. The first filter is applied to strip out mixtures that have a critical temperature T_{crit} lower than 210 °C (see Figure 2b)). This is to cover the uncertainty range of the mixture critical temperature calculation to avoid transcritical operation of the cycle. After the application of the first filter, 21,796 mixtures are left in the pool. Next up, a filter on vapor pressure $p_{vap}^{25°C}$ > 50 kPa is applied and it filters out the most of the mixtures (627 mixtures left), as is presented in Figure 2c). Finally as shown in Figure 2d), the last filter removes mixtures which have a compressor discharge temperature T_5 above 220 °C (32 mixtures left). When sorting these resulting mixtures by 2nd law efficiency η_{2nd}, all of them land in the above 0.5 region. Although acetone was initially considered in the pure components list, the results for mixtures containing acetone were finally discarded because the gains were only marginal compared to the "best" mixtures that do not include acetone. The "best" ternary mixture then, likely as well more chemically stable and less toxic and prone to fractionation than mixtures with acetone fraction, consists of cyclopentane+R1336mzz(Z)+R1233zd(E) with mole fractions of [0.72,0.24,0.04], respectively. Following the same procedure, the "best" binary and quaternary mixtures are selected and compared in Table 3 with pure cyclopentane, which is the main component of all the "best" blends.

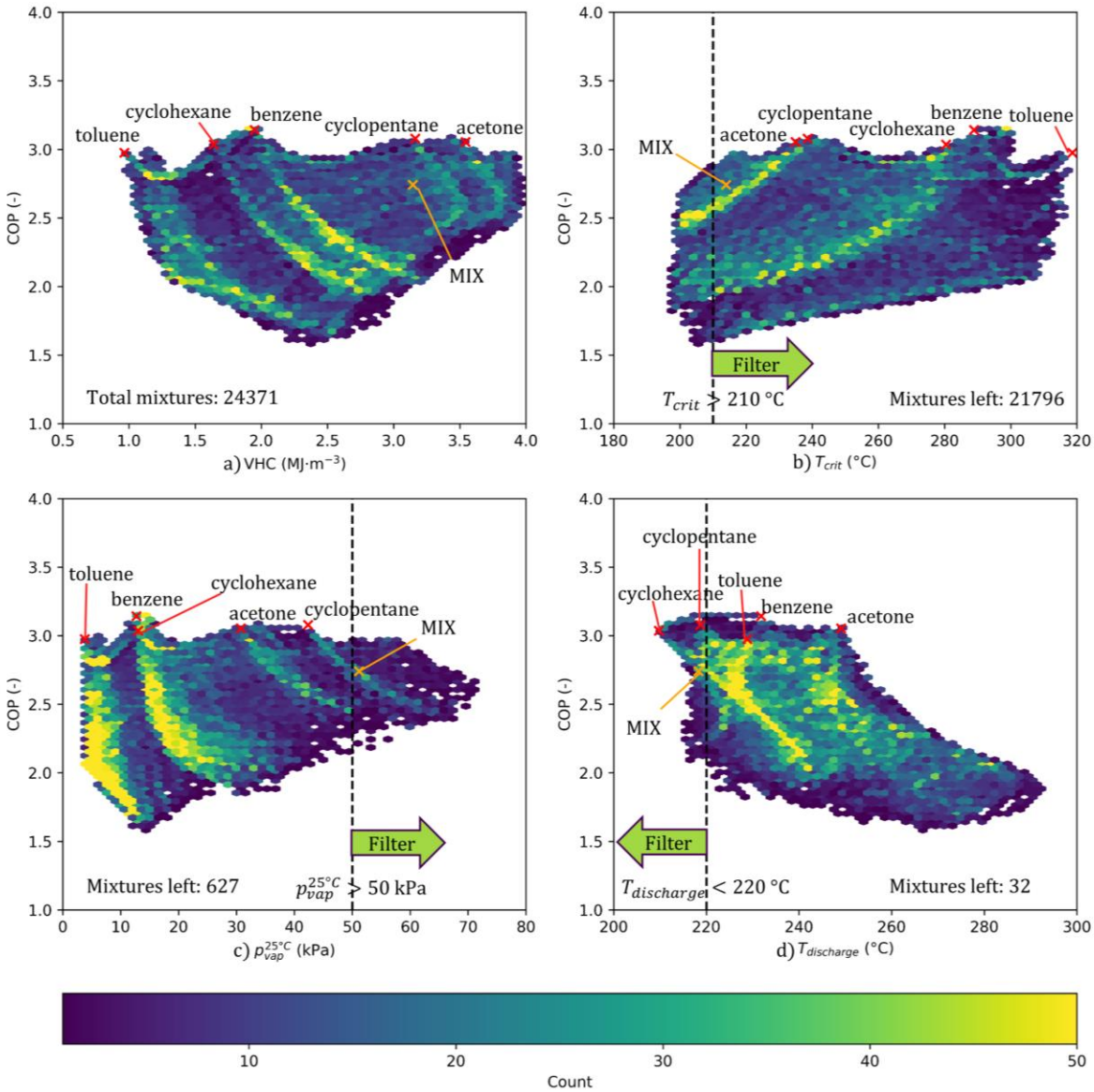

Figure 2 Mixture screening results, hexbin histograms for ternary mixtures; COP as a function of a) VHC, b) mixture critical temperature, c) mixture vapor pressure, d) compressor discharge temperature; MIX = cyclopentane&R1336mzz(Z) [0.68,0.32] molar fractions

Table 3 Comparison of pure cyclopentane and "best" binary, ternary and quaternary mixtures

Parameter	pure fluid	binary mixture	ternary mixture	quaternary mixture
fluids	cyclopentane	cyclopentane, R1336mzz(Z)	cyclopentane, R1336mzz(Z), R1233zd(E)	cyclopentane, R1336mzz(Z), R1233zd(E), R1224yd(Z)
mole fractions (-)	1.0	0.68,0.32	0.72,0.24,0.04	0.64,0.28,0.04,0.04
COP (-)	3.08	2.74	2.77	2.66
η_{2nd} (Carnot | Lorenz) (-)	0.532 | 0.477	0.503 | 0.445	0.508 | 0.450	0.503 | 0.443
T_5 (°C)	218.68	218.28	219.60	219.88
$p_{vap}^{25°C}$ (kPa)	42.34	51.16	50.47	53.80
T_{crit} (°C)	238.57	213.92	216.89	210.57

Noticeably, the differences between the "best" mixtures are small (relative difference in η_{2nd} between the "best" binary and the "best" ternary is less than 0.01). Taking that into consideration, the binary mixture of cyclopentane+R1336mzz(Z) with molar fraction of 0.68 and 0.32 respectively is selected as "the best of the best" for the given case, boundary conditions and filtering method. The ternary and quaternary mixtures were not obviously superior to the two-component mixture described above, though we include this analysis for completeness. Sorting the mixtures according to the 2nd law efficiency η_{2nd} defined using COP_{Lorenz} instead of COP_{Carnot} yields qualitatively same results for the winning candidates, however shifted towards lower absolute values.

3.2 Mixture Flammability Estimation Results

As for the flammability estimation model results, Figure 3 showcases the strong tendency of the mixtures to land into the "A2&A3" region (23,178 mixtures) compared to the A2L region (1,348 mixtures). Actually, all of the 32 mixtures that passed all the filters by the screening method are situated within the "A2&A3" region. Although this method can't distinguish between an A2 and A3 fluid due to the limitations of the existing data extracted from ASHRAE Standard 34 submissions, generally speaking it is more likely that the mixture will be an A2 classified, if the fluorine loading is higher at the same adiabatic flame temperature. The flammability of the selected mixture is yet to be determined by an experimental method.

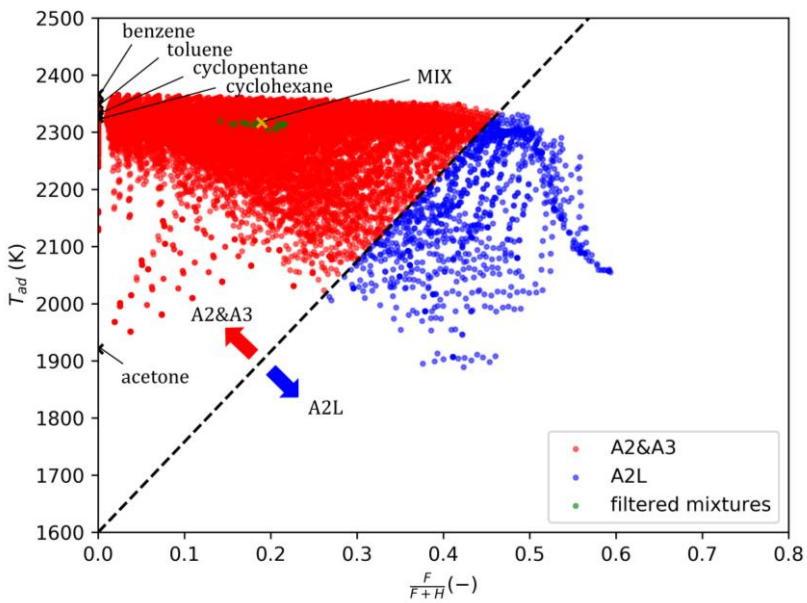

Figure 3 Flammability estimation of the screened mixtures; MIX = cyclopentane&R1336mzz(Z) [0.68,0.32] molar fractions

4. DISCUSSION OF THE RESULTS

Ultimately, we were not successful in the hunt for a blend that meets all of our desired criteria as none of the mixtures that survived the imposed constraints was estimated to be classified as "mildly flammable" (A2L) by the ASHRAE Standard 34. We think that blending a cyclic hydrocarbon and an HFO is a way to achieve a mixture representing a good compromise in most of the criteria in the design space and accept the A2&A3 flammability estimation of the preferred mixture. For both components of the mixture, there are experimental data for thermal and chemical stability with positive results of up to 250 °C in the presence of aluminum, copper, carbon steel, moisture and air. (Ginosar et al., 2011; Kontomaris, 2014) None of the A2L classified mixtures pass the vapor pressure filter and the discharge temperature filter, all of them are very high temperature glide mixtures with significant differences in NBP, which may lead to a risk of fractionation of the mixture.

The cycle model was simplified, and several assumptions were used for a smooth and fast calculation procedure with a wide range of mixtures. On the cycle model level, the highest uncertainty arises from the compressor efficiency model, which is very preliminary and not corresponding to the screw compressor that will be ultimately utilized. This

efficiency model is quite pessimistic and penalizes high pressure ratios. We also applied the most pessimistic scenario of the boundary conditions selection in terms of saturation state points which disfavors high glide mixtures. For example, the way the internal heat exchanger is modelled is again the least favorable from the efficiency point of view, as already superheated vapor inlets to the IHX and the outlet superheat is not controlled to provide optimal compressor inlet conditions. Intermediate pressure level is a geometrical mean value of evaporating and condensing pressure as a simple preliminary estimate which saves computational resources without significantly harming the accuracy of the screening.

Working fluid mixture thermodynamic and transport properties are not a simple juxtaposition of EOS of each component, but an additional term in the EOS specific for the blend needs to be determined. For the blends investigated here, as these are uncommon mixtures whose properties have yet not been experimentally obtained and their interaction parameters fitted, an estimation model is applied to achieve these mixture specific EOS coefficients (most importantly the interaction parameter γ_T). (E. Lemmon & McLinden, 2001) From this estimation method stems the greatest uncertainty in calculating the mixture properties. (Bell et al., 2019) reported that an uncertainty of 5% of γ_T as a conservative estimate of the mixing parameter results roughly in less than a 2% uncertainty in COP calculation and about 18% of the VHC calculation. These results, however, should not affect the selection of the preferred mixture. The uncertainty analysis of the flammability model was reported in detail in the original work of (Linteris et al., 2019).

5. CONCLUSIONS AND FUTURE WORK

This paper presents a methodology to select a multi-component working fluid consisting of hydrocarbons and H(C)FOs for an industrial HTHP for process heat delivery at 200 °C temperature level and discusses the results obtained for a given set of boundary conditions and cycle architecture, which will be used in an experimental test rig.

In total, over 460,000 mixtures of hydrocarbons and H(C)FOs created from the fluids in Table 1 were explored. Most of the mixtures failed a simple test of $T_{crit} > T_{cond}$; those who passed were used in simulation of an advanced HTHP VCC model and the results were analyzed, filtered and sorted to find the most suitable blend based on user-imposed criteria for an experimental investigation as a next step. Flammability estimation model shown that all of the mixtures that were filtered were estimated to be A2 or A3 classified (flammable or highly flammable). Comparing the best blends, only marginal gains were identified for more complex mixtures. Therefore, a mixture of cyclopentane and R1336mzz(Z) of molar fractions of 0.68 and 0.32 respectively, is the choice of preference for the case study. Ultimately, working fluid selection is always a question of trade-offs in terms of thermodynamic performance, safety considerations, environmental concerns, oil compatibility and costs. We invite a fellow reader to use the provided script for their own search for the "best" blend for their case. (Spale et al., 2024b)

Future work on this matter will include experimental measurement of the thermodynamic mixture properties to determine the BIPs and we will explore how the HTHP model performance changes when using the experimental BIPs, compared to the real system performance and to the current results of the mixture screening using estimated BIPs from REFPROP 10. The conclusions of this work provide a basis to further experimentally investigate industrial HTHP with screw compressor operating with low GWP mixtures for up to 200 °C heat supply. There are, however, still many challenges to overcome towards a successful laboratory prototype unit, such as oil miscibility, thermal decomposition and chemical interaction of the lubricant and working fluid, effect of thermal losses and pressure drops to the system design, thermal management of the compressor and design of the vapor injection.

NOMENCLATURE

Variables

h	Specific enthalpy (kJ·kg^{-1})
p	Pressure (kPa)
q	Specific heating capacity (kJ·kg^{-1})
Q	Heating capacity (kW)
s	Specific entropy (kJ·(kg·K)$^{-1}$)
T	Temperature (°C)
w	Specific work (kJ·kg^{-1})
x	Quality (-)

Subscripts

ad	Adiabatic flame
Carnot	Carnot
crit	Critical
comp	Compressor

cond	Condenser
discharge	Compressor discharge
eco	Economizer
ev	Evaporator
freez	Freezing
HS	High-pressure stage
lift	Temperature lift
LS	Low-pressure stage
Lorenz	Lorenz
in	Inlet condition
IHX	Internal heat exchanger
is	Isentropic
max	Maximum
min	Minimum
obj	Objective state
out	Outlet condition
SC	Subcooled
SH	Superheat
sink	Heat sink
source	Heat source
split	Split flow
th	Thermal
vap	Saturated vapor
vol	Volumetric
2nd	Second law
100	100 years (CO_2-equivalent)

Greek alphabet

α	Non-dimensional mass flow rate
γ	Interaction parameter
Δ	Difference
η	Efficiency
π	Pressure ratio
ρ	Density

Abbreviations

CFC	Chlorofluorocarbons
COP	Coefficient of performance
EOS	Equation of state
GWP	Global warming potential
HP	High pressure
HTHP	High temperature heat pump
HFO	Hydrofluoroolefin
HC	Hydrocarbon
HCFC	Hydrochlorofluorocarbon
HCFO	Hydrochlorofluoroolefin
HFC	Hydrofluorocarbon
IHX	Internal heat exchanger
LP	Low pressure
ODP	Ozone depletion potential
TSECOIHX	Two-stage cycle with economizer and internal heat exchanger
VCC	Vapor-compression cycle
VHC	Volumetric heat capacity
WHR	Waste heat recovery

ACKNOWLEDGEMENT

This material is based upon work supported by the U.S. Department of Energy's Office of Energy Efficiency and Renewable Energy (EERE) under the Industrial Efficiency & Decarbonization Office, Award Number DE-0010864. This work was partially funded by The National Institute of Standards and Technology (NIST), an agency of the United States Department of Commerce and by the Grant Agency of the Czech Technical University in Prague, grant No. SGS24/087/OHK2/2T/12. Jan Spale gratefully acknowledges support for this publication by the J.W. Fulbright Commission Czech Republic. Its contents are solely the responsibility of the author and do not necessarily represent the official views of the Fulbright Program.

DISCLAIMER

REFERENCES

Abedini, H., Vieren, E., Demeester, T., Beyne, W., Lecompte, S., Quoilin, S., & Arteconi, A. (2023). A comprehensive analysis of binary mixtures as working fluid in high temperature heat pumps. *Energy Conversion and Management*, *277*, 116652. https://doi.org/10.1016/j.enconman.2022.116652

ASHRAE. (2022). *ANSI/ASHRAE Standard 34-2022—Designation and safety classification of refrigerants*.

Bell, I. H., Domanski, P. A., McLinden, M. O., & Linteris, G. T. (2019). The hunt for nonflammable refrigerant blends to replace R-134a. *International Journal of Refrigeration*, *104*, 484–495. https://doi.org/10.1016/j.ijrefrig.2019.05.035

Fernández-Moreno, A., Mota-Babiloni, A., Giménez-Prades, P., & Navarro-Esbrí, J. (2022). Optimal refrigerant mixture in single-stage high-temperature heat pumps based on a multiparameter evaluation. *Sustainable Energy Technologies and Assessments*, *52*, 101989. https://doi.org/10.1016/j.seta.2022.101989

Ganesan, P., & Eikevik, T. M. (2023). New zeotropic CO2-based refrigerant mixtures for cascade high-temperature heat pump to reach heat sink temperature up to 180 °C. *Energy Conversion and Management: X*, *20*, 100407. https://doi.org/10.1016/j.ecmx.2023.100407

Gao, C. W., Allen, J. W., Green, W. H., & West, R. H. (2016). Reaction Mechanism Generator: Automatic construction of chemical kinetic mechanisms. *Computer Physics Communications*, *203*, 212–225. https://doi.org/10.1016/j.cpc.2016.02.013

Ginosar, D. M., Petkovic, L. M., & Guillen, D. P. (2011). Thermal Stability of Cyclopentane as an Organic Rankine Cycle Working Fluid. *Energy & Fuels*, *25*(9), 4138–4144. https://doi.org/10.1021/ef200639r

Goodwin, D. G., Speth, R. L., Moffat, H. K., & Weber, B. W. (2021). *Cantera: An Object-oriented Software Toolkit for Chemical Kinetics, Thermodynamics, and Transport Processes*. https://doi.org/10.5281/zenodo.4527812

Kontomaris, K. (2014). *HFO-1336mzz-Z: High Temperature Chemical Stability and Use as A Working Fluid in Organic Rankine Cycles*. International Refrigeration and Air Conditioning Conference (Paper ID:1525). https://docs.lib.purdue.edu/iracc/1525

Lemmon, E., & McLinden, M. (2001, November 1). *Method for Estimating Mixture Equation of State Parameters*.

Lemmon, E. W., Bell, I. H., Huber, M. L., & McLinden, M. O. (2018). *NIST Standard Reference Database 23: Reference Fluid Thermodynamic and Transport Properties-REFPROP, Version 10.0, National Institute of Standards and Technology*. https://doi.org/10.18434/T4/1502528

Linteris, G. T., Bell, I. H., & McLinden, M. O. (2019). An empirical model for refrigerant flammability based on molecular structure and thermodynamics. *International Journal of Refrigeration*, *104*, 144–150. https://doi.org/10.1016/j.ijrefrig.2019.05.006

Mateu-Royo, C., Arpagaus, C., Mota-Babiloni, A., Navarro-Esbrí, J., & Bertsch, S. S. (2021). Advanced high temperature heat pump configurations using low GWP refrigerants for industrial waste heat recovery: A comprehensive study. *Energy Conversion and Management*, *229*, 113752. https://doi.org/10.1016/j.enconman.2020.113752

multiprocessing—Process-based parallelism. (2024, January 28). Python Documentation. https://docs.python.org/3/library/multiprocessing.html

Obika, E., Heberle, F., & Brüggemann, D. (2024). Thermodynamic analysis of novel mixtures including siloxanes and cyclic hydrocarbons for high-temperature heat pumps. *Energy*, *294*, 130858. https://doi.org/10.1016/j.energy.2024.130858

pandas documentation—Pandas 2.2.1 documentation. (2024, February 23). https://pandas.pydata.org/docs/

scipy.optimize.minimize—SciPy v1.12.0 Manual. (2024, January 20). https://docs.scipy.org/doc/scipy/reference/generated/scipy.optimize.minimize.html

Spale, J., Hoess, A. J., Bell, I. H., & Ziviani, D. (2024a). *Exploratory Study on Low-GWP Working Fluid Mixtures for Industrial High Temperature Heat Pump with 200 °C Supply Temperature* (SSRN Scholarly Paper 4784217). https://doi.org/10.2139/ssrn.4784217

Spale, J., Hoess, A. J., Bell, I. H., & Ziviani, D. (2024b). *Supplementary materials—Exploratory Study on Low-GWP Working Fluid Mixtures for Industrial High Temperature Heat Pump with 200°C Supply Temperature—Mendeley Data* [dataset]. Mendeley data. https://doi.org/10.17632/t75kdftzyv.1

World Meteorological Organization (WMO). (2022). *Scientific Assessment of Ozone Depletion: 2022* (GAW Report No. 278; p. 509). WMO.